Available online at www.sciencedirect.com

SCIENCE DIRECT®

Infrared Physics & Technology 46 (2005) 493–505

INFRARED PHYSICS & TECHNOLOGY

www.elsevier.com/locate/infrared

Corrugated waveguide band edge filters for CMB experiments in the far infrared

E. Gleeson [a,*], J.A. Murphy [a], B. Maffei [b], W. Lanigan [a], J. Brossard [c], G. Cahill [a], E. Cartwright [a], S.E. Church [d], J. Hinderks [d], E. Kirby [d], C. O'Sullivan [a]

[a] *Department of Experimental Physics, NUI Maynooth, Co. Kildare, Ireland*
[b] *University of Wales, Cardiff, CF24 3YB, UK*
[c] *CNES, Centre Spatial de Toulouse, 18, Avenue Edouard Belin, 31 401 Toulouse Cedex 4, France*
[d] *Stanford University, Stanford, CA 94305, USA*

Received 16 August 2004
Available online 15 December 2004

Abstract

Millimetre wave corrugated waveguide-horn structures are used as both single-moded and multi-moded bolometer feeds in a number of cosmic microwave background (CMB) experiments (e.g. PLANCK, Archeops, QUaD). Such horns tend to be employed over a relatively wide bandwidth and for single-moded horns the waveguide acts as the high pass filter. In this paper we report on our investigation on how the waveguide details determine the exact location of the low frequency band edge of such corrugated horns. A sharp step-like band edge, below which there is negligible propagation, is ideally required. Furthermore any leakage below the expected cut-off, possible in corrugated guides, could lead to non-idealised cross-polar effects. Typically deeper corrugations are required in the waveguide filter than at the horn aperture for wide bandwidth operation, thus necessitating a transition section over which the corrugation depth smoothly varies. An electromagnetic mode matching technique and a surface impedance hybrid mode model are used to compute the horn transmission characteristics. We have also undertaken laboratory measurements of the band edge of prototype corrugated horns in order to test the models.

JEL classification: 95.55.−n; 95.55.Cs; 95.55.Fw; 07.87.+v

Keywords: Band edge; Filters; CMB; Corrugated horns

* Corresponding author. Tel.: +353 1 7084674; fax: +353 1 7083313.
E-mail address: emily.m.gleeson@may.ie (E. Gleeson).

1350-4495/$ - see front matter
doi:10.1016/j.infrared.2004.10.001

1. Introduction to CMB horn design

Millimetre wave corrugated waveguides and horn antenna structures of circular cross-section are used as detector feeds on both the High Frequency Instrument (HFI) on the European Space Agency PLANCK surveyor satellite telescope [1–3] and on the ground based QUaD telescope [4]. Such waveguide structures have the advantage that they can transmit both orthogonal polarisations of any possible circular modes and are therefore very efficient for bolometric systems. They are also relatively easy to manufacture compared with the standard rectangular horns. The use of a corrugated waveguide to feed the horn increases the structure's efficiency and bandwidth, and also produces a sharper band edge than if the waveguide was smooth walled with a transition to corrugated guide in the horn. PLANCK, which is due to be launched in 2007, will map the temperature and polarisation anisotropies of the CMB over the entire sky with unprecedented sensitivity and angular resolution [5]. In 2005 QUaD [4] will commence its observations from the DASI (Degree Angular Scale Interferometer) mount at the South Pole and is optimised for measurements of the polarisation properties of the CMB.

For single-moded horns the corrugated waveguide acts as a high pass filter. Optical filters are necessary to define the high frequency band edge and to this end hot pressed polypropylene filters [6] will be used in the PLANCK-HFI and QUaD detector systems. A back-to-back corrugated horn antenna design, as shown in Fig. 1(a) has been adopted for feeding the bolometric detectors on the HFI. The bandwidth defining filters can thus be placed between the back-to-back horns and the bolometer-module feeds, ensuring no degradation of the horn beam patterns coupled to the telescope. Single-moded Gaussian profiled horns have been developed for the four lowest frequency channels (100 GHz, 143 GHz, 217 GHz and 353 GHz) on the HFI [1]. Four horns at each of these frequencies will be used for polarisation measurements and each channel contains two orthogonally orientated polarisation selective bolometers (PSBs) [7] which detect both polarisations of the incoming radiation separately. The remaining single-moded horns and all of the multi-moded horns are coupled to polarisation non-selective bolometers. The QUaD telescope is coupled to a single array of single-moded corrugated horn antenna feeds (100 GHz and 150 GHz) via front-end optics (Fig. 1(b)) with the low pass filters mounted at the front of the horn antennas. These horns are also coupled to two orthogonally orientated PSBs.

Powerful in-house software (National University if Ireland, Maynooth), *SCATTER2*, based on a rigorous electromagnetic mode matching technique was developed for accurate modelling of these horns. In the electromagnetic mode matching technique [2,8] a corrugated waveguide or horn structure is regarded as a sequence of circular waveguide segments with the radius stepping between the top and bottom of the corrugation slots as in Fig. 2(a). The natural modes of propagation for each segment are the *TE* and *TM* modes of a uniform circular waveguide. At the interface between two segments, the power carried by the individual incident modes is scattered between the backward propagating reflected modes in the first guide segment and the forward propagating modes in the second guide segment as illustrated

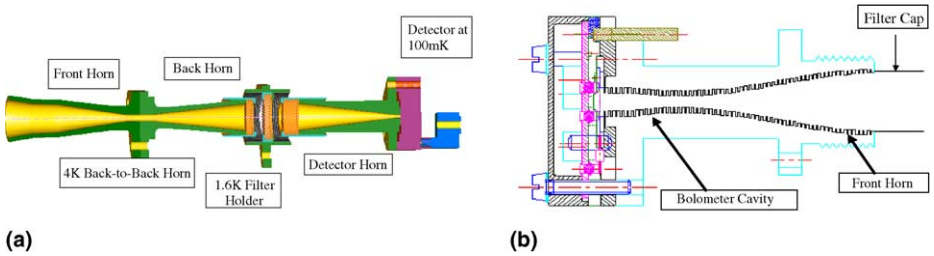

Fig. 1. (a) PLANCK detector configuration and (b) QUaD detector configuration.

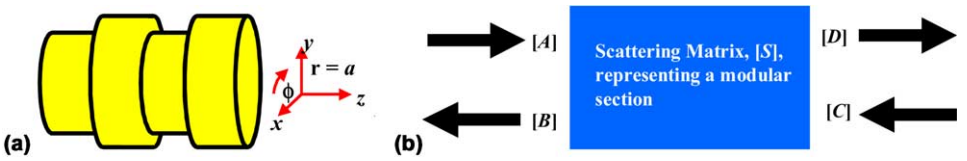

Fig. 2. (a) Corrugated horn antenna illustrating the cylindrical co-ordinate system for waveguides and horn antennas of circular cross-section and (b) the scattering matrix, [*S*], for a modular section of a horn antenna or waveguide which relates the coefficients on the input side (left) to the coefficients on the output side (right).

in Fig. 2(b). The technique is based on matching the total transverse field in the two guides at the junction, so that the total complex power is conserved. Track must also be kept of the evanescent modes in the guide as these can propagate as far as the next step in the profile for short segments. The relationship between the input and output mode coefficients for each junction between sections is described by a scattering matrix. Modal propagation between junctions can be expressed as a diagonal matrix whose elements describe the phase evolution of the modes. The matrices are then cascaded section by section to obtain an overall scattering matrix for the horn structure.

An alternative approach for modelling the propagation characteristics inside corrugated horns involves the use of hybrid modes. This is based on an average surface impedance approximation [9] and is valid for corrugated circular waveguides provided that there are many corrugations per wavelength. The corrugated "walls" can be regarded as having a uniform surface impedance defined by E_z and H_ϕ. This approach is fast and reasonably accurate for computing transmission properties and does not involve scattering matrices but directly uses eigensolutions of a transcendental equation arising from the Helmholtz equation

$$\nabla^2\mathbf{E} + k^2\mathbf{E} = 0 \tag{1}$$

where $k^2 = k_c^2 + \beta^2$ (waveguide equation) [8]. $k = 2\pi/\lambda$ is the free space wavenumber, k_c is the transverse waveguide wavenumber and β is the axial propagation factor. Solutions for $k_c = \chi/a$ (where the χ coefficient depends on the particular hybrid mode and a is the waveguide radius) are found by matching the surface admittance [9] at $r = r_i$ (Fig. 4). Thus, the hybrid mode approach is particularly useful in the design of the waveguide filters, as it is straightforward to predict mode cut-off effects in the waveguide sections, in terms of the waveguide radius and the slot depths.

In this paper we concentrate on the factors that are important in the design of the waveguide filter section of back-to-back horns. We also discuss the so called transition section (over which the corrugation depth changes from its value in the waveguide to that in the horn). As examples we take the PLANCK-HFI and QUaD horns, designed to meet the various demanding restrictions imposed by the complex focal plane layouts. Much of the development of the single-moded horns for the PLANCK-HFI concentrated on optimising the 143 GHz channel and in fact, the precise waveguide filter dimensions of the horns were the last parameters to be finalised. Prior to this various prototype models with different horn profiles were investigated and experimentally verified, initially concentrating on optimising the beam pattern quality particularly with respect to sidelobe reduction at the band centre [1]. Another critical issue for the horns was the position of the phase centre behind the horn aperture [3]. Before commencing the work on the details of the waveguide filter section, a so called prototype "profiled-flare" design (as shown in Fig. 3) had already been approved for the single-moded HFI horn antennas [1,10].

In Section 2 we discuss how the mode matching and hybrid mode techniques were applied in order

Fig. 3. General geometry of the PLANCK-HFI single-moded profiled flared cylindrically symmetric corrugated horn antennas.

to model propagation in specific corrugated waveguide designs. The PLANCK-HFI and QUaD horns were required to have a 33% bandwidth and therefore for the 143 GHz horns on the HFI (on which most of this paper focuses) this corresponds to a low frequency band edge of 119 GHz. To achieve the desired band edge involved optimising the performance of the waveguide section. The design process was quite involved, as a sharp step-like band edge was required with no low frequency propagation below this edge. Section 3 outlines the effect that the waveguide transition sections have on the quality of the low frequency band edge of a corrugated horn. Experimental measurements of the band edge of the 100 GHz QUaD horn and the 150 GHz *P01* prototype HFI horn are reported in Section 4. Such measurements are crucial to assessing the accuracy and limitations of the models, particularly if numerical instabilities are possible in computational software codes.

2. Band edge for corrugated waveguide filters

Modelling the filtering properties of a corrugated waveguide is a complex issue and can be understood either in terms of hybrid modes [2,9] or waveguide mode scattering [2,8] as explained in the introduction. The size of the waveguide determines the number of independent modes that can propagate in the waveguide-horn system. It also determines the effective band edge as the exact physical dimensions of the corrugations affect the frequency bandwidth of the modes, both in terms of their low frequency cut-on and high frequency cut-off points. In particular the high frequency cut-off is a unique feature of hybrid modes not encountered in smooth walled waveguides [9]. Ideally only the HE_{11} mode should propagate for optimum horn performance.

2.1. Hybrid mode model: HE_{11} mode cut-off and EH_{11} mode leakage

As an example we take the 143 GHz horn antenna for the PLANCK-HFI system as shown in Fig. 4. The corrugation depth switches from 0.4λ in the waveguide to 0.25λ (or $\lambda/4$) at the horn aperture based on the central design frequency of 143 GHz (free space wavelength, $\lambda = 2.098$ mm). The $\lambda/4$ corrugation depth at the horn aperture is required in order to obtain balanced hybrid modes (and therefore symmetric beam patterns on the sky with low cross-polarisation levels). The 0.4λ depth in the waveguide corrugations increases the bandwidth of the horn. This is shown in the HE_{11} and EH_{11} modal dispersion curves in Fig. 5 which are parameterised in terms of r_i/r_o, the ratio of the waveguide inner radius (to the top of the corrugation grooves) to the waveguide outer radius (to the bottom of the grooves), with kr_i as abscissa, where as usual $k = 2\pi/\lambda$. The range of kr_i (and therefore range of frequencies) over which only the HE_{11} mode is transmitted is greater for much lower val-

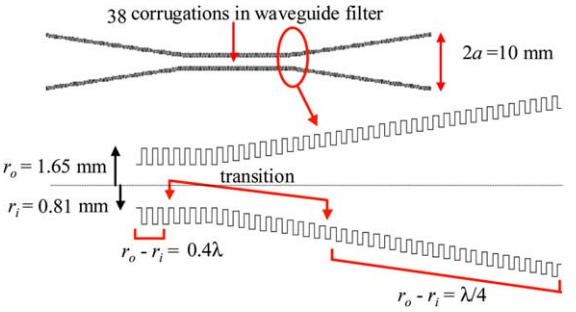

Fig. 4. Conical corrugated horn antenna with a waveguide inner and outer radius of 0.81 mm and 1.65 mm respectively.

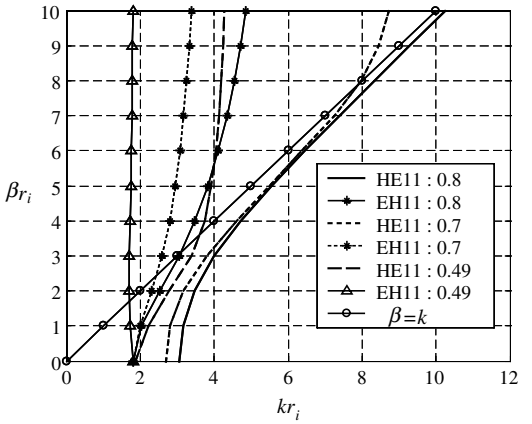

Fig. 5. Dispersion curves for the EH_{11} and HE_{11} modes for $r_i/r_o = 0.49$, 0.7, 0.8. Modes reach their high frequency cut-off above the $\beta = k$ line.

ues of r_i/r_o in the waveguide than those required at the horn aperture (see Fig. 5), e.g. the range of kr_i between $r_i/r_o = 0.49$ (in the waveguide, for example) and $r_i/r_o = 0.8$ (at the horn aperture, for example) is much greater than the transmitted frequency range when $r_i/r_o = 0.7$ in the waveguide (i.e. shallow corrugations). Such deep corrugations are also required to suppress the EH_{11} mode which can scatter into the HE_{11} mode if the corrugations in the waveguide filter are too shallow. For $r_i/r_o = 0.49$ in the waveguide filter section there is no overlap between the dispersion curves of both modes. However, as r_i/r_o increases to 0.7 and 0.8, the range of frequencies at which both modes can in theory coexist also increases so that modal scattering is possible.

Using a hybrid mode approach it is possible to determine the predicted bandwidth of the modes using the low frequency and high frequency hybrid mode cut-off point charts [2]. Some examples are shown in Fig. 6 for low order modes. In the waveguide of the sample horn in Fig. 4 where $r_i/r_o = 0.49$, the EH_{11} mode is above its low frequency cut-off (Fig. 6(a)) when $kr_i > 1.8$ ($v = 106$ GHz) and is below its high frequency cut-off (Fig. 6(b)) when $kr_i < 1.93$ ($v = 114$ GHz). Similarly, the HE_{11} mode cuts on when $kr_i = 1.88$ ($v = 111$ GHz).

The actual HE_{11} and EH_{11} low frequency cut-offs can also be estimated using the following arguments. At the low frequency cut-off point the HE_{11} mode behaves like a TM_{11} mode [9] in a waveguide defined by the radius r_o to the bottom of the slot and its cut-off wavelength is given as

$$\lambda_c = \frac{2\pi r_o}{3.8317}. \tag{2}$$

Similarly, an EH_{11} mode behaves like a TE_{11} mode [9] in a smooth-walled waveguide of radius r_i and its cut-off wavelength is given by

$$\lambda_c = \frac{2\pi r_i}{1.8412}. \tag{3}$$

The hybrid mode model is useful therefore as it can accurately predict the modes that can exist in the waveguide. Although the EH_{11} mode can have significant power in the waveguide, it becomes evanescent in the horn and most of its power is reflected at the throat of the horn. This can been seen in Fig. 5. For a balanced hybrid mode (linearly polarised symmetric beam pattern) $r_o - r_i \approx \lambda/4$ at the horn aperture. Therefore, for a horn with $r_i\lambda$ at the aperture $r_i/r_o \geqslant 0.8$ and $kr_i > 6$. The dispersion curve for the EH_{11} mode tends towards infinity at $kr_i > 6$ (i.e. the mode has reached its high frequency cut-off) and the wide gap between the EH_{11} and HE_{11} dispersion curves in the waveguide therefore removes the possibility of scattering between the modes before reaching the horn aperture region. Thus we expect negligible power below the HE_{11} fundamental hybrid mode low frequency cut-on i.e. below 111 GHz in this case.

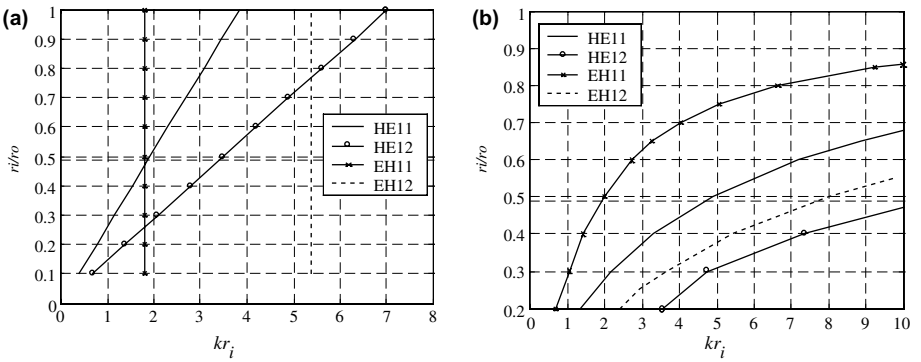

Fig. 6. (a) Low frequency and (b) high frequency cut-off charts for the EH_{11}, EH_{12}, HE_{11} and HE_{12} modes. The horizontal line intersects the modal propagation curves at $r_i/r_o = 0.49$.

2.2. Mode matching model: azimuthal order $n = 1$ cut-off

The second approach used to determine the band edge involves the use of the scattering matrix technique (*SCATTER2* software). The elements of the scattering matrices represent the amplitude mode coefficients at the output of the system for a mode of unit complex power at the input to the system, and can be used to determine the total power at the horn aperture as a function of frequency. Underlying the technique is the assumption that the field, E, can be expressed as a linear sum of modes (e_i) as given by equation

$$\mathbf{E} = \sum_i a_i \mathbf{e}_i \tag{4}$$

with an infinite number of modes required to obtain a perfect description of the field. However, for numerical and computational reasons a finite number of modes is in fact used.

The concept of complex power, P, carried by a mode is defined as $P = \int \mathbf{E} \times \mathbf{H}^* \mathrm{d}S$. The power transmitted for modes of azimuthal order $n = 1$, corresponding to hybrid HE_{11} and EH_{11} modes, for the horn in Fig. 4 is shown in Fig. 7 where scattering matrices were used in the computation. Using this approach there appears to be EH_{11} mode propagation between 103 and 109 GHz. While the EH_{11} mode is only above its $\bar{\beta} = 0$ "low frequency cut-off" at 106 GHz (using the hybrid approach), the low frequency leakage between 103 and 106 GHz (using scattering matrices) can clearly also be attributed to the EH_{11} mode. We can see this from the dispersion curves for the EH_{11} and HE_{11} modes for $r_i/r_o = 0.49$ shown in Fig. 8. The vertical lines represent frequencies of 102 GHz, 106 GHz (band edges for EH_{11} propagation) and 114 GHz (HE_{11} cut-on).

Significant power below the HE_{11} band edge is unexpected when the corrugation depths in the waveguide filter are sufficiently deep as argued in the previous section. The transmission as a function of frequency was therefore computed using scattering matrices with limited mode sets of different sizes. In this example 20×20, 30×30 and 40×40 element matrices were used in the simulations where a 20×20 matrix implies 10 TE and 10 TM modes. We expect that the 40×40 case will be more accurate which suggests that there is no significant leakage as shown in Fig. 7. However, the strong dependence of the mode matching technique on the number of modes used indicates that it is computationally unstable at certain frequencies below the HE_{11} band edge. Therefore power may still be transmitted in this region although at a much lower level than above the HE_{11} band edge. This was investigated experimentally and the results are reported in Section 4.

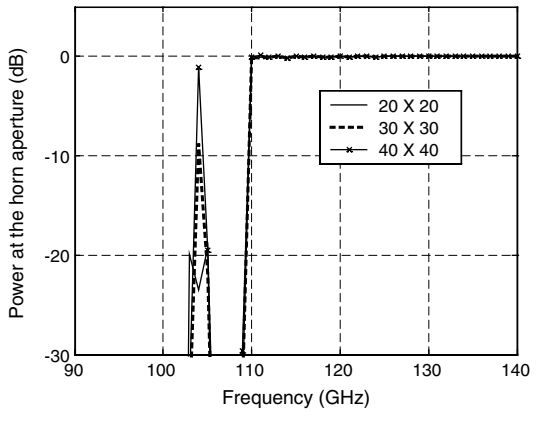

Fig. 7. Azimuthal order $n = 1$ transmission for the conical corrugated horn in Fig. 5 computed using scattering matrices (i.e. the *SCATTER2* software).

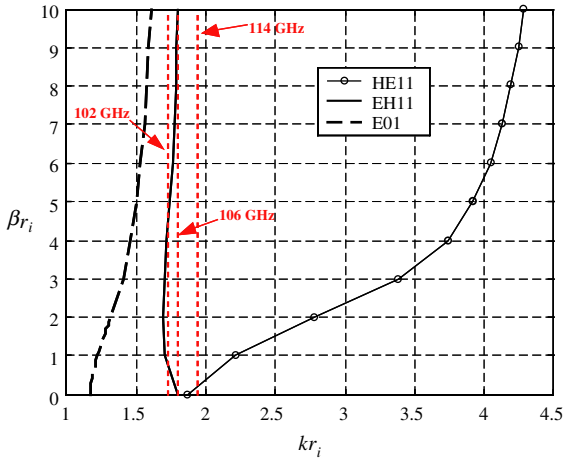

Fig. 8. Dispersion curves for the HE_{11}, EH_{11} and E_{01} modes for $r_i/r_o = 0.49$.

To summarise, the scattering matrix approach can predict the frequency range of the EH_{11} leakage but cannot accurately predict the magnitude of the power in this mode below the HE_{11} band edge. This is because some of the matrices become quasi-singular due to the finite number of modes used in the analysis. On the other hand, at frequencies above the HE_{11} band edge the transmitted power predicted is independent of the basis mode set size. The technique is therefore computationally stable in this region. It is worth noting the impressive consistency between both the hybrid mode and scattering matrix models in predicting a HE_{11} band edge around 111 GHz.

2.3. Modes of azimuthal order $n = 0$

According to both the hybrid mode and scattering matrix models, the E_{01} hybrid mode can also exist below the HE_{11} band edge. For the horn in Fig. 4, this mode is predicted to propagate between 70 GHz and 103 GHz. However, as can be seen in Fig. 8, this mode behaves in a similar manner to the EH_{11} mode as it approaches its high frequency cut-off almost as soon as it cuts on. Using scattering matrices this mode also suffers from the same computational instabilities as the EH_{11} mode. The mode can have power in the waveguide but it becomes evanescent in the horn and most of its power is reflected before it reaches the horn aperture. It cannot scatter into the HE_{11} mode (because the modes have different azimuthal symmetry) and as a result its power at the horn aperture is negligible as will again be discussed in Section 4 in the case of experimental verification of the models.

3. Effect of the waveguide and transition region details on the HE_{11} band edge

As already discussed in the previous section the corrugation depths in the waveguide need to be deeper than those at the horn aperture. It is therefore necessary to have a transition region in the corrugated structure over which the corrugation depth varies smoothly in order to prevent modal scattering. It turns out that the transition needs very careful design to ensure no leakage below the HE_{11} cut-off, the problem being that the EH_{11} mode can scatter in the transition and the throat of the horn. This transition can be placed within the waveguide, in the horn outside the waveguide or alternatively can span the horn throat region where the guide and horn sections meet. The transition region was in the horn in the example considered in the previous section (Figs. 4 and 7).

The horn designs discussed in this section are similar to the prototype 143 GHz HFI horn in Fig. 4 where $r_i = 0.81$ mm, $r_o = 1.65$ mm and $r_i/r_o = 0.49$, with the deep corrugations necessary to suppress the EH_{11} mode. The remainder of this section concentrates on how the required band edge, with a sharp step-like cut-on profile is dependent on the details of the transition. The bandwidth plots illustrated in this section were computed using the scattering matrix approach. The hybrid mode model predicts a HE_{11} band edge at 111 GHz.

3.1. Transition (from deep to shallow corrugations) in horn profile

In Section 2 we showed that the band edge is sharp and step-like for a sample horn where the transition from deep to shallower corrugations begins at the first corrugation outside the waveguide filter section. As a first example we consider 143 GHz PLANCK-HFI prototype conical horn designs which have six corrugations (short waveguide) and 38 corrugations (long waveguide), respectively. In these examples the transition extends over 20 corrugations and it is observed that the HE_{11} band edge is step-like for both of these horns but is sharper for the horn with the longer waveguide as shown in Fig. 9.

The effect of the number of corrugations in the actual horn transition was investigated next. The remaining horns considered have 10 corrugations in their waveguide filter sections. It is clear from Fig. 10(a) that the band edge has a better step-like definition with low ringing when the transition extends over 20 corrugations rather than 10 corrugations. As mentioned in Section 2 using the hybrid mode approach the EH_{11} mode is predicted to

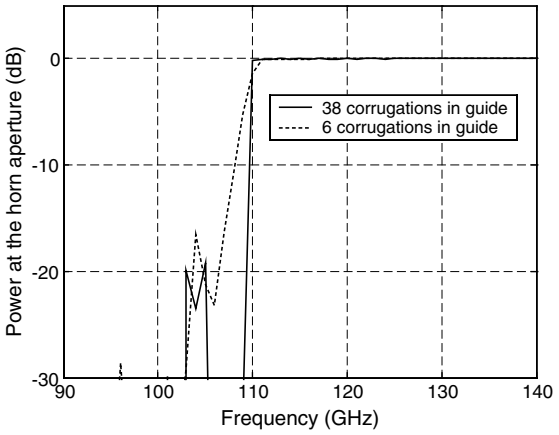

Fig. 9. Effect of the number of corrugations in the waveguide on the $n = 1$ transmission.

propagate at frequencies in the range 106–114 GHz and the HE_{11} mode cuts on at 111 GHz. The scattering matrix approach also predicts some low frequency leakage of the EH_{11} mode as shown in Fig. 10(a) although as previously discussed, this is likely to be due to numerical instabilities and the power is expected to be negligible. This will be discussed further when experimental data are presented in Section 4.

The horn design was then modified to the profiled flared geometry required by HFI where the waveguide dimensions are $r_i = 0.754$ mm, $r_o = 1.539$ mm, $r_i/r_o = 0.49$ which moves the band edge to the required 119 GHz as shown in Fig. 10(b). In addition the transition in the new design started three corrugations from the waveguide section. This clearly results in a well defined step-like band edge as required, suggesting that starting the transition a few corrugations into the horn results in a better design. Note that for the two cases shown in Fig. 10(b) different band edges were predicted due to the different waveguide dimensions.

3.2. Transition (from deep to shallow corrugations) in waveguide

When the corrugation depth transition begins in the waveguide filter section the sharp step-like HE_{11} band edge profile is replaced by an edge with unstable ringing as shown in Fig. 11. As in the previous subsection we consider conical geometries with 38 (long waveguide) and 52 (very long waveguide) corrugations in the waveguide sections but here the transition from deep to shallow corrugations begins within the waveguide filter section and spans the horn throat region. The scattering matrix approach predicts some low frequency leakage of the EH_{11} mode as shown in Fig. 12 and clearly the most striking effect is that the band edge (neglecting the power at lower frequencies) is not step-like. This can be attributed to the change in corrugation depths actually occurring in the waveguide because the transition section extends into the waveguide. In this case varying the number of corrugations in the waveguide filter section has a negligible effect on the horn transmission properties.

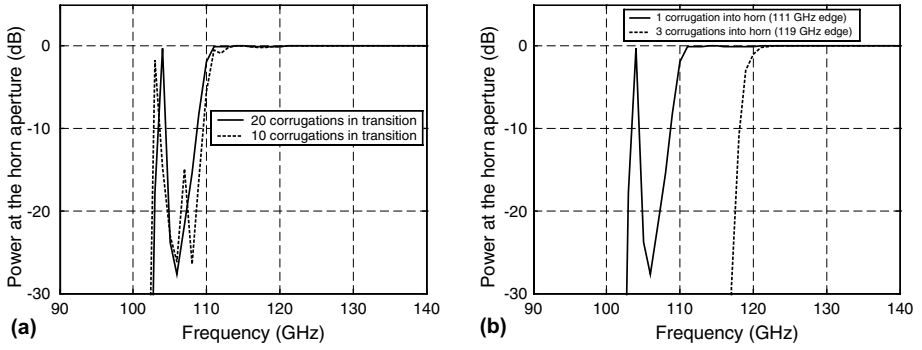

Fig. 10. (a) Effect of the number of corrugations in the transition and (b) the position of the transition relative to the waveguide filter (the band edge moves as the waveguide dimensions are $r_i = 0.81$ mm, $r_o = 1.65$ mm (for the solid curve) and $r_i = 0.754$ mm $r_o = 1.539$ mm (for the dashed curve)) on the $n = 1$ transmission.

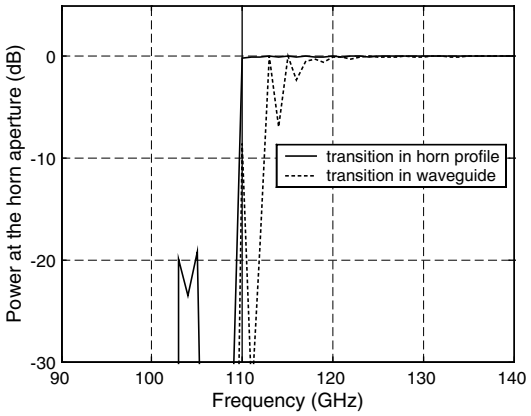

Fig. 11. Effect of the position of the transition on the $n = 1$ horn transmission.

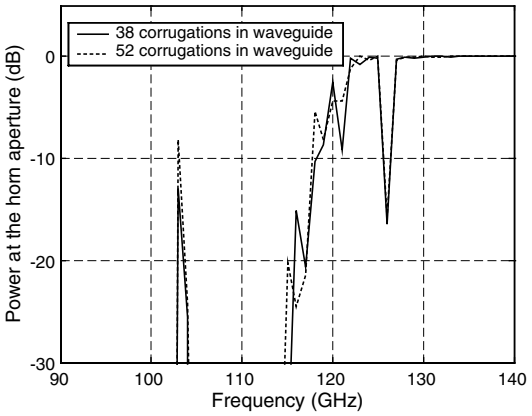

Fig. 12. Effect of the number of corrugations in the waveguide on the $n = 1$ transmission.

It was also important to check whether the horn details affect the leakage of the EH_{11} mode, by allowing the mode to scatter into the propagating HE_{11} mode. Furthermore it was also important to check that the flare section at the front of the profiled horn was not contributing to the overall transmission characteristics of the horn as the sharp increase in the profile diameter could result in scattering effects interacting with the throat region. Reassuringly, the presence of the flare does not appear to contribute to the ringing on the profile at the HE_{11} band edge. The main effect that the flare has is on the power in the EH_{11} mode as shown in Fig. 13(a). However, this also possibly results from the unstable nature of the computations in the high scatter regime of the EH_{11} mode. In addition, the prediction that the normalised power transmission exceeds unity is clearly unphysical. Measurements of the *P01* horn were taken at the University of Wales, Cardiff to support this assertion and other recent measurements discussed in Section 4 also indicate that the computed power is unstable and overestimated below the HE_{11} band edge. These results are very reassuring, as any significant leakage below the expected cut-off would lead to non-idealised cross-polar effects in any sensitive CMB experiments.

The third comparison involves the number of corrugations in the horn transition region. We only in fact consider the cases with 15 and 17 corrugations. Because the transition began in the waveguide, the azimuthal order $n = 1$ (HE_{11}) band edge is still uneven (Fig. 13(b)) but there is however a noticeable improvement for the case with 17 corrugations rather than 15, which again suggests some resonance ringing effects especially as

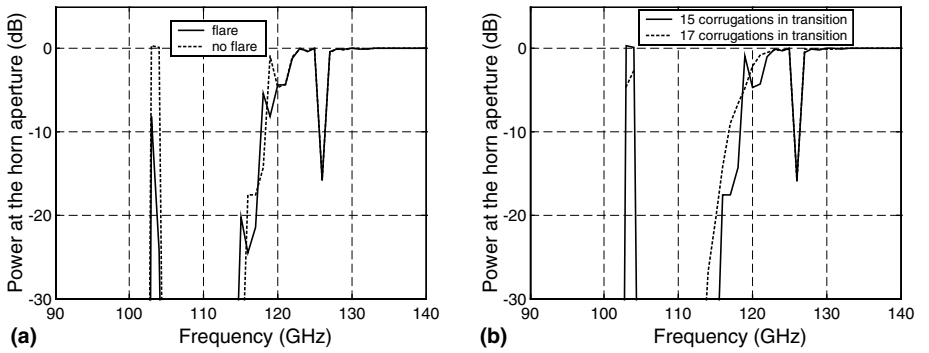

Fig. 13. Effect of: (a) the horn flare and (b) the number of corrugations in the transition region on the $n = 1$ transmission.

we would not expect much difference for such similar numbers of corrugations.

To summarise the conclusion of this section, the outer (deeper) radius of the waveguide essentially determines the HE_{11} band edge [2] (see Eq. (2)). A sharp step-like band edge can be achieved by beginning the transition outside the waveguide section. The sharpness of the band edge can be further improved by either increasing the number of corrugations in the waveguide or increasing the number of corrugations in the transition. By beginning the transition a few corrugations from the waveguide filter section the band edge approaches a step function. On the other hand if the transition begins in the waveguide the HE_{11} band edge is not sharp but instead shows ringing effects. However there is some noticeable improvement when the number of corrugations in the transition is tuned, which suggests some resonance effects.

4. Bandwidth edge measurements for CMB waveguide filters

In this section excellent agreement between the theoretically predicted and experimentally measured HE_{11} band edge is shown for both the 150 GHz *P01* prototype PLANCK-HFI horn and also for the 100 GHz QUaD horn. In Sections 2 and 3 we showed that below the HE_{11} band edge the scattering matrix model suffers from some computational instabilities: this being evidenced by the unphysical prediction of the greater than unity power fraction transmitted and also by the strong dependence of the transmitted power on the number of modes used in the finite computation. Thus, in addition to proving that the band edge is located where it is theoretically expected to be, the measurements were also necessary to determine the level of low frequency leakage of the EH_{11} and E_{01} modes, if any, below the HE_{11} band edge.

4.1. On-axis transmission of the P01 corrugated conical horn for the HFI

On-axis transmission measurements of the *P01* conical corrugated horn antenna, shown in Fig. 14, were undertaken at the University of Wales, Cardiff, using an experimental set-up with a backward wave oscillator (BWO) as the source of millimetre radiation. This source was linearly polarised, via a corrugated horn and a single-moded rectangular waveguide, and the measurement was repeated using a twisted waveguide in order to rotate the polarisation of the radiation by 90°. In the set-up the source horn was located on-axis in the far field of the back-to-back horn under investigation, which in turn fed a cryogenically cooled bolometer located inside a cryostat. In the measurements taken, the on-axis gain was recorded as a function of frequency. In order to normalise the power and determine the fractional transmission, the measurements were then repeated for both source polarisations without the presence of the *P01* horn in front of the bolometer feed. Fig. 15 compares the experimental data to the scattering matrix model prediction using modes of azimuthal order 1 only.

The experimental HE_{11} band edge is at 125 GHz which agrees perfectly with the *SCATTER2* mode-matching and hybrid mode predictions. Clearly, the experimentally measured on-axis power below the HE_{11} mode band edge is negligible (of the order of 0.25% of the power

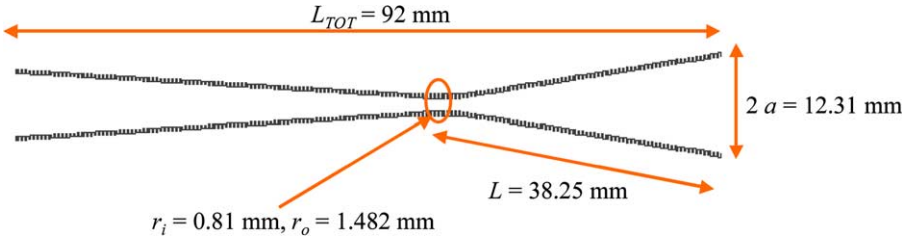

Fig. 14. Geometry of the *P01* corrugated conical horn antenna.

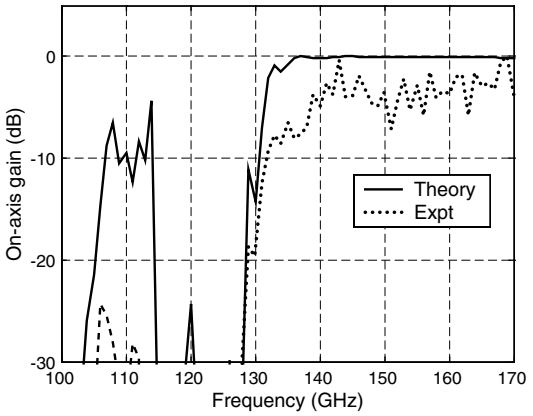

Fig. 15. $n = 1$ transmission in the *P01* horn: experimental data versus the scattering matrix prediction.

in the HE_{11} mode) which is consistent with the fact that below this band edge the $n = 1$ scattering matrix technique suffers from some numerical instabilities. Nevertheless the scattering matrix prediction is still useful as it seems to predict the slightly enhanced transmission range for the EH_{11} mode between 105 and 112 GHz, although the power involved is of course negligible at the horn aperture compared to the HE_{11} transmission.

4.2. On-axis transmission of the 100 GHz QUaD horn

The band edge of the 100 GHz QUaD horn, shown in Fig. 16, was measured at the National University of Ireland (NUI), Maynooth [11] and also at Stanford University. The experimental set-up at NUI Maynooth involved the use of a tunable Gunn oscillator and a chopping reference signal was applied to both the Gunn oscillator power supply and the lock-in amplifier in order to discriminate between background noise and the true signal. Again in this case, the on-axis power was recorded as a function of frequency in a similar set-up to that described in the previous section. However, a Golay cell, which is polarisation insensitive, was used instead of a bolometer in these measurements. Again the predicted and measured HE_{11} band edges agree perfectly as shown in Fig. 17(a). In order to ensure that there was no unexpected off-axis power being transmitted, beam patterns were also measured at regular frequency intervals below cut-off [11]. In particular these measurements observed no unusual off-axis beam pattern behaviour in the reflection region of the EH_{11} and E_{01} modes below the HE_{11} band edge. The *SCATTER2* software was also capable of computing far field beam patterns at all frequencies.

Band edge measurements at Stanford University were also made on this horn but in this case using a Fourier transform spectrometer (FTS). In this set-up a liquid nitrogen cold load was used as a blackbody radiation source at 77 K with a chopper wheel providing an alternating signal using a second blackbody source at 300 K. A beam-splitter sent radiation to both a movable and a fixed mirror and the re-combined interfering radiation was reflected into the QUaD test bed

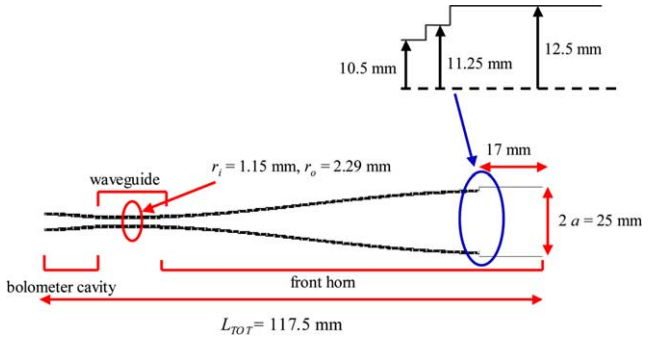

Fig. 16. Final design of the 100 GHz QUaD horn.

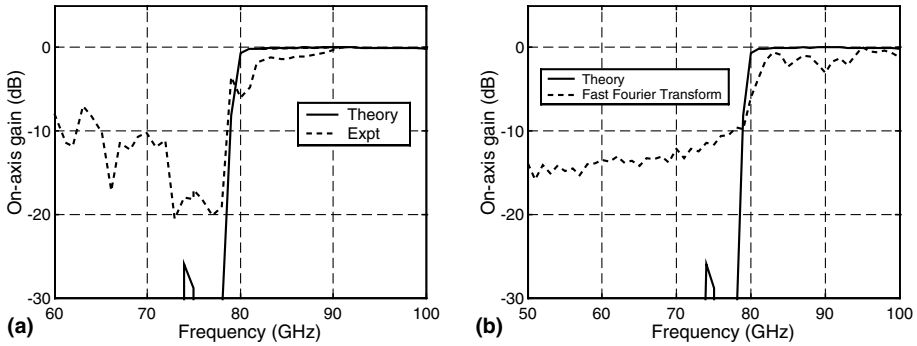

Fig. 17. (a) Measured and predicted band edge of the QUaD 100 GHz horn (NUI Maynooth) and (b) fast Fourier transform (FFT) and predicted band edge of the QUaD 100 GHz horn (Stanford University).

(300 mK fridge). The optical path length difference was $x = 2\Delta L$, where ΔL was the difference between the two path lengths. A fast Fourier transform of the measured interferogram yielded the QUaD transmission data shown in Fig. 17(b). The poor rejection of noise in the FTS system impaired the sensitivity of the measurements but clearly the correct band edge performance with low leakage below the edge was again recorded.

5. Conclusions

We have presented a summary of the principal issues involved in the development of band edge corrugated waveguide filters which satisfy the demanding design and analysis required for the detector feed horns in CMB experiments, in particular the ESA PLANCK Surveyor satellite and the ground-based telescope QUaD. The aim is to achieve a horn design which has a sharp step-like HE_{11} band edge with negligible low frequency leakage, which would lead to undesirable results, such as increased cross-polar levels. The excellent agreement between the scattering matrix predictions and experimental measurements of the band edge was demonstrated. The predicted and measured transmission agree for frequencies greater than the HE_{11} low frequency cut-off but the EH_{11} leakage characteristics are not possible to accurately characterise using this approach because for some frequency regimes the scattering matrices become quasi-singular below the HE_{11} band edge so that the technique becomes numerically unstable.

Acknowledgments

The authors wish to acknowledge the financial assistance of Enterprise Ireland, the Irish Research Council for Science and Technology: IRCSET (Embark award) and the National University of Ireland Maynooth (Daniel O'Connell Fellowship).

References

[1] B. Maffei et al., Shaped corrugated horns for cosmic microwave background anisotropy measurements, Int. J. Infrared Millimetre Waves 21 (2000) 2023.
[2] J.A. Murphy et al., Radiation patterns of multi-moded corrugated horns for far-IR space applications, Infrared Phys. Technol. 42 (2001) 515.
[3] E. Gleeson et al., 'Phase centres' of far infrared multi-moded horn antennas, Int. J. Infrared Millimetre Waves 23 (5) (2002) 711–730.
[4] S. Church et al., QUEST and DASI: a south-pole CMB polarisation experiment, New Astron. Rev. 47 (2003) 1083–1089.
[5] J.M. Lamarre et al., The high frequency instrument on PLANCK: Design and performance, Astro Lett. Commun. 37 (2000) 161–170.
[6] P.A.R. Ade, Tucker, C., Haynes, C.V., Filters, dichroics, beam dividers and Fabry–Perot plates for ultra-low-background far infrared instruments, in: Proceedings of the

Second Workshop on New Concepts for Far-IR Submillimeter Space Astronomy, March 7–8, 2002, University of Maryland, 2002.
[7] J.J. Bock, Bolometers for millimeter-wave cosmology, in: Proceedings of the 2K1BC Workshop on Experimental Cosmology at Millimetre Wavelengths, Breuil Cervinia, Italy, July 2001.
[8] A.D. Olver et al., Microwave Horns and Feeds, IEEE Press, New York, 1994 (Chapter 4).
[9] P.J.B. Clarricoats, A.D. Olver, Corrugated Horns for Microwave Antennas, Peter Peregrinus, 1984 (Chapter 3).
[10] R. Colgan, Electromagnetic and quasi-optical modelling of horn antennas for far-IR space applications, Ph.D. thesis, Maynooth 2001.
[11] J.A. Murphy et al., Millimetre-wave Profiled Corrugated Horns for the QUaD CMB Polarisation Experiment, Toshitaka Idehara (Ed.), Int. J. Infrared Millimetre Waves, 2004, submitted.